Geophysical Research Letters

RESEARCH LETTER
10.1029/2017GL076854

Key Points:
- We use palinspastic geometry of the preextensional Sevier orogen and critical Coulomb wedge (CCW) theory to infer the friction coefficient μ_D of the Sevier Desert detachment (SDD)
- Compressive CCW theory suggests μ_D values of 0.2–0.24 for thrust faults when crustal shortening ceased in the early Paleocene
- A decrease of SDD dip from a maximum of 30° to present-day inclination of 11° and extensional CCW theory implies that μ_D decreased to 0.13

Correspondence to:
X. P. Yuan,
xyuan@gfz-potsdam.de

Citation:
Yuan, X. P., Christie-Blick, N., & Braun, J. (2018). Mechanical properties of the Sevier Desert detachment: An application of critical Coulomb wedge theory. *Geophysical Research Letters*, *45*. https://doi.org/10.1029/2017GL076854

Received 19 DEC 2017
Accepted 5 APR 2018
Accepted article online 19 APR 2018

Mechanical Properties of the Sevier Desert Detachment: An Application of Critical Coulomb Wedge Theory

X. P. Yuan[1], N. Christie-Blick[2], and J. Braun[1]

[1]Helmholtz Centre Potsdam, German Research Centre for Geosciences (GFZ), Potsdam, Germany, [2]Department of Earth and Environmental Sciences, Lamont-Doherty Earth Observatory, Columbia University, Palisades, NY, USA

Abstract Low-angle normal faults are widely regarded as playing an important role in crustal extension. Among the most influential examples, the Sevier Desert detachment (SDD) has been imaged in seismic reflection profiles beneath the Sevier Desert basin of west-central Utah. An extensional offset of as much as 47 km is thought to have occurred since the late Oligocene at or near its present dip of 11°. We use the palinspastic geometry of the preextensional Sevier orogen and critical Coulomb wedge (CCW) theory to constrain the friction coefficient, μ_D of the inferred detachment. It is assumed that the SDD is at least in part a reactivated strand of the Pavant thrust system. Compressive CCW theory suggests μ_D values of 0.2–0.24 for thrust faults when crustal shortening ceased in the early Paleocene. A decrease in the dip of the SDD from a maximum of 30° to its present-day inclination of 11° and extensional CCW theory implies that μ_D decreased from 0.2–0.24 initially to 0.13 today. Salt, for which the normal-stress dependence of the friction equation disappears with even shallow burial, is widespread in the Sevier Desert basin and presents locally also in Jurassic strata of central Utah. Elevated pore fluid pressure may have played a role in reducing the effective normal stress. Our model can be tested directly by coring across the detachment and by measuring material properties and the pore fluid pressure in the vicinity of the contact.

Plain Language Summary Low-angle normal faults are widely regarded as playing an important role in crustal extension. Among influential examples, the Sevier Desert detachment is of broad interest because for more than 40 years it has represented a benchmark of detachment. We use a generally accepted palinspastic geometry of preextensional Sevier orogen and critical Coulomb wedge theory to investigate friction coefficients that may have existed along the Sevier Desert detachment during both compressional thrusting and subsequent extension. Our model can be tested by coring across the detachment and by measuring material properties and pore fluid pressure. Resolving the origin of this feature will have far-reaching implications for mechanisms of crustal extension.

1. Introduction

Low-angle normal faults (LANFs) are widely regarded as playing an important role in crustal extension and the development of rifted continental margins (e.g., Axen, 2004; Lister et al., 1991; Manatschal et al., 2007; Wernicke, 1985; Whitney et al., 2013). Andersonian theory predicts that within the brittle upper crust in extensional settings, newly formed normal faults are optimally inclined at 60°–65° for most rock types and internal friction coefficients of 0.6–0.85 (Byerlee, 1978). Not yet fully resolved is whether or under what conditions normal faults may have slipped at low inclination (<25°–30°; Collettini & Sibson, 2001; Collettini, 2011; Forsyth, 1992; Mesimeri et al., 2018; Sibson, 1985) or whether the orientation of such faults is due largely to tilting during deformation, with or without the development of a rolling hinge (Axen & Bartley, 1997; Buck, 1988; Jackson & White, 1989; Proffett, 1977; Wernicke & Axen, 1988; Whitney et al., 2013).

One of the earliest and most influential reported examples of an upper crustal LANF is located beneath the Sevier Desert of west-central Utah (Figure 1a) and is referred to as the Sevier Desert detachment (SDD; Allmendinger et al., 1983; Christie-Blick et al., 2009; DeCelles & Coogan, 2006; Niemi et al., 2004; McBride et al., 2010; Von Tish et al., 1985). The SDD is thought by some to have reactivated the preextensional Pavant thrust (PVT) and to root into the lower crust to the west of the Sevier Desert (Figure 1a; DeCelles & Coogan, 2006; cf. Allmendinger et al., 1983; Anders et al., 2001, 2012; Christie-Blick et al., 2007; Stahl & Niemi, 2017; Wills et al., 2005). The extensional offset is inferred to be as great as 47 km since the late Oligocene at or near its present dip of 11° (DeCelles & Coogan, 2006; Von Tish et al., 1985). The inferred scale and palinspastic geometry of the SDD is incompatible with both domino and rolling hinge models.

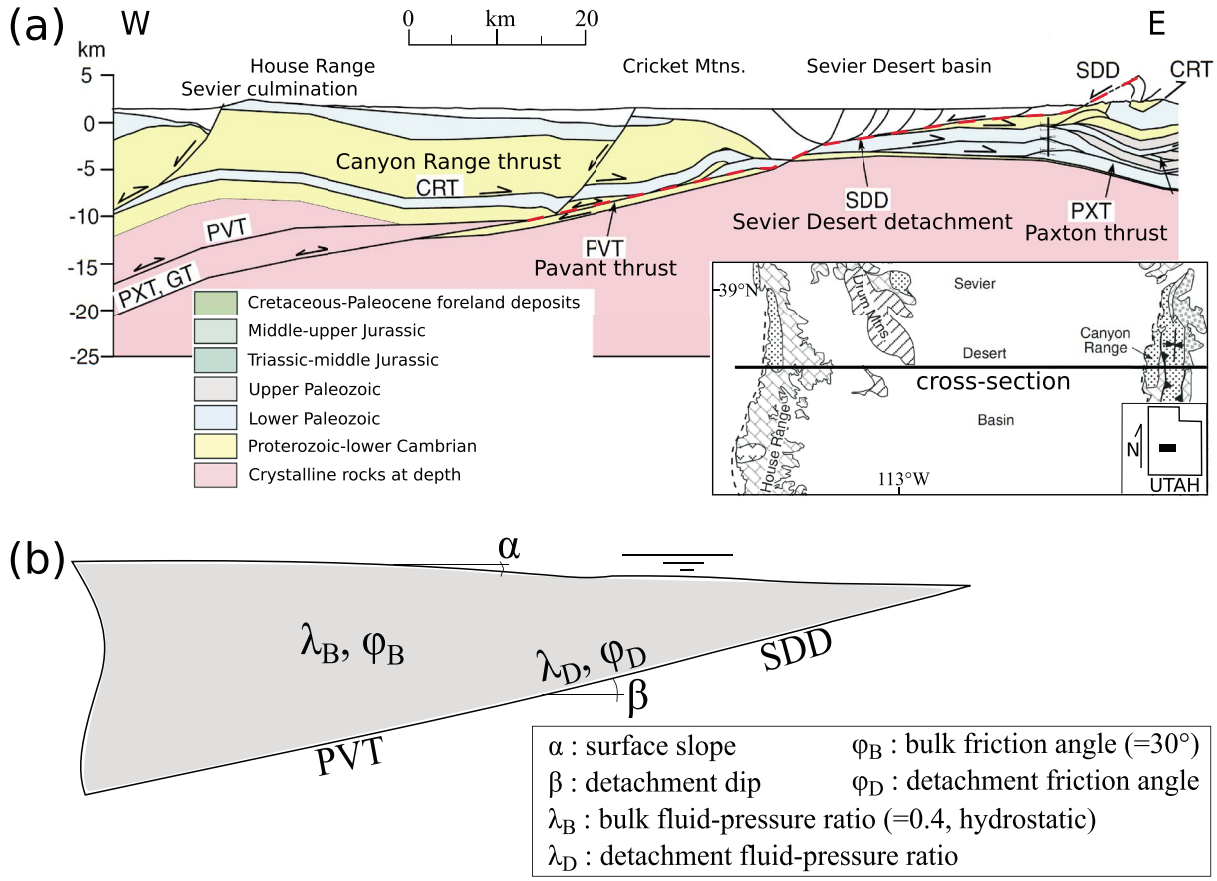

Figure 1. (a) Regional cross section of the Sevier Desert detachment (SDD), adopted from DeCelles and Coogan (2006). The legend refers to this figure and to Figure 2a. (b) Simplified prototype to represent wedge above SDD and PVT (red dashed curve in a) for using the CCW theory. The detachments (SDD and PVT) are currently inclined at $\beta = 11°$.

The purpose of this paper is to place constraints on the mechanical properties of the SDD using the critical Coulomb wedge (CCW) theory of Davis et al. (1983) and Dahlen (1984). We assume the widely accepted structural and palinspastic interpretation of DeCelles and Coogan (2006) as a point of departure. Alternative interpretations of details, so long as they include the SDD, make little difference to our analysis at the scale of interest. CCW theory has been used extensively to investigate accretionary and orogenic wedges, including the Sevier orogen in Utah (DeCelles & Mitra, 1995). The extensional version of this theory (Xiao et al., 1991) is applied here for the first time in this same geology.

2. Critical Coulomb Wedge Theory in Compressive and Extensional Settings

CCW theory was developed in the context of orogens and accretionary wedges and by analogy with the deformation of sand in front of a moving bulldozer (Dahlen, 1984; Davis et al., 1983). The main result of the theory is that a subcritical wedge deforms internally by thrusting (or folding) until the surface slope is increased sufficiently to make the wedge critical in shape (on the verge of internal deformation everywhere). For the wedge at the critical shape, sliding occurs along the basal décollement without internal thrusting. The geometry of the wedge (surface slope α and décollement dip β) depends on the friction angles φ_B of wedge bulk material and φ_D for the décollement and the fluid pressure ratios λ_B and λ_D within the bulk material and on the décollement, respectively. The λ ranges between ρ_f/ρ (fluid density/saturated rock density) and 1. The noncohesive CCW theory (Dahlen, 1984), corrected by Yuan et al. (2015) for fluid overpressured cases, gives the critical slope α_c from the following relations:

$$\alpha_c + \beta = \Psi_D - \Psi_O, \tag{1}$$

$$\Psi_D = \frac{1}{2}\arcsin\left[\left(\frac{1-\lambda_D}{1-\lambda_B}\right)\frac{\sin(\varphi_D)}{\sin(\varphi_B)} + \left(\frac{\lambda_D-\lambda_B}{1-\lambda_B}\right)\sin(\varphi_D)\cos(2\Psi_O)\right] - \frac{1}{2}\varphi_D, \quad (2)$$

$$\Psi_O = \frac{1}{2}\arcsin\left(\frac{\sin(\alpha_c')}{\sin(\varphi_B)}\right) - \frac{1}{2}\alpha_c', \quad (3)$$

$$\alpha_c' = \arctan\left[\left(\frac{1-\rho_f/\rho}{1-\lambda_B}\right)\tan(\alpha_c)\right], \quad (4)$$

where Ψ_D is the angle between the maximum principal stress σ_1 and the basal décollement and Ψ_O is the angle between σ_1 and the topographic surface.

Xiao et al. (1991) broadened CCW theory to extensional settings. Extensional wedges overlying detachments are characterized by normal rather than reverse slip on the detachment. A subcritically tapered wedge, with $\alpha > \alpha_c$, will fail by normal faulting, thereby reducing its taper until it reaches the critically tapered shape. A critically or supercritically tapered wedge is stable and therefore can slide on a detachment without normal faulting. The critical slopes of the extensional wedges can be obtained from the compressive CCW theory by simply replacing φ_D in equation (2) with the value of $-\varphi_D$.

3. Geometry From Cross Section of DeCelles and Coogan (2006)

The region of what is now the Sevier Desert basin experienced thrusting in the Late Cretaceous and extension beginning in the late Oligocene or Miocene (DeCelles & Coogan, 2006). We assume the pre-Cenozoic geometry shown in Figure 8, panel F, of DeCelles and Coogan (2006) as a point of departure, a widely accepted interpretation, though we acknowledge that more than one view exists about how the specific thrust faults project to depth (e.g., Anders et al., 2012). Thrust faults become younger to the east. The Gunnison thrust (GT) is both the youngest and structurally lowest fault, which uses the same basal décollement inclined at β_D as other thrusts (Figure 2a). The Canyon Range thrust (CRT) is in the upper plate of the Pavant thrust (PVT), of which there are several strands. The upper Paleozoic and Mesozoic rocks make up the upper crustal wedge. Wedge geometry above the basal décollement (critical, because of thrusting everywhere) and compressive CCW theory provide an excellent constraint on the frictional properties of the décollement. The décollement dip $\beta_D = 4°$, with uncertainty 0.3°, and the average surface slope $\alpha = 1.7°$, with uncertainty 0.3°, were determined from the pre-Cenozoic structure shown in Figure 2a. The assumed surface slope is consistent with two paleoelevation estimates of Gregory-Wodzicki (1997) for the late Eocene (?) House Range flora (3.6 ± 0.7 km and 2.9 ± 1.5 km).

The structural geometry at the time extension began and the initial dip β_0 of the SDD are also implied. A careful comparison of Figures 1a and 2a indicates how the SDD needs to be drawn at the time of the earliest slip. Some segments of the SDD correspond to strands of the PVT. Other segments are new fault surfaces with dips as great as $\beta_0 \sim 30°$ at the topographic surface. We can distinguish and keep track of the SDD, as illustrated by red dashed curve in Figure 2a. The initial SDD and PVT are assumed to have the same friction coefficient as the basal décollement. It is also reasonable to assume that the Paleozoic and Mesozoic rocks imbricated by thrusting at criticality reflect the same internal friction angle as Cenozoic sedimentary rocks extended at criticality during SDD activity.

A difficulty in this region is that many kilometers of the orogenic wedge were eroded during crustal shortening. The preserved record of deformation is therefore incomplete. Thrusting tends to increase the surface slope α before wedge reaching a critical shape, whereas surface processes lead to a decrease in the surface slope. Variation of α provides a constraint on values of SDD friction angle φ_D. Additionally, the Sevier Desert basin reflects a combination of crustal thinning and isostatic rebound. A first-order implication of displacement on the SDD is footwall uplift that would necessarily reduce the inclination of the detachment. Such uplift has been assumed since the work of Allmendinger et al. (1983) to account for the culmination of crystalline rocks beneath the Sevier Desert. Synextensional sedimentation would

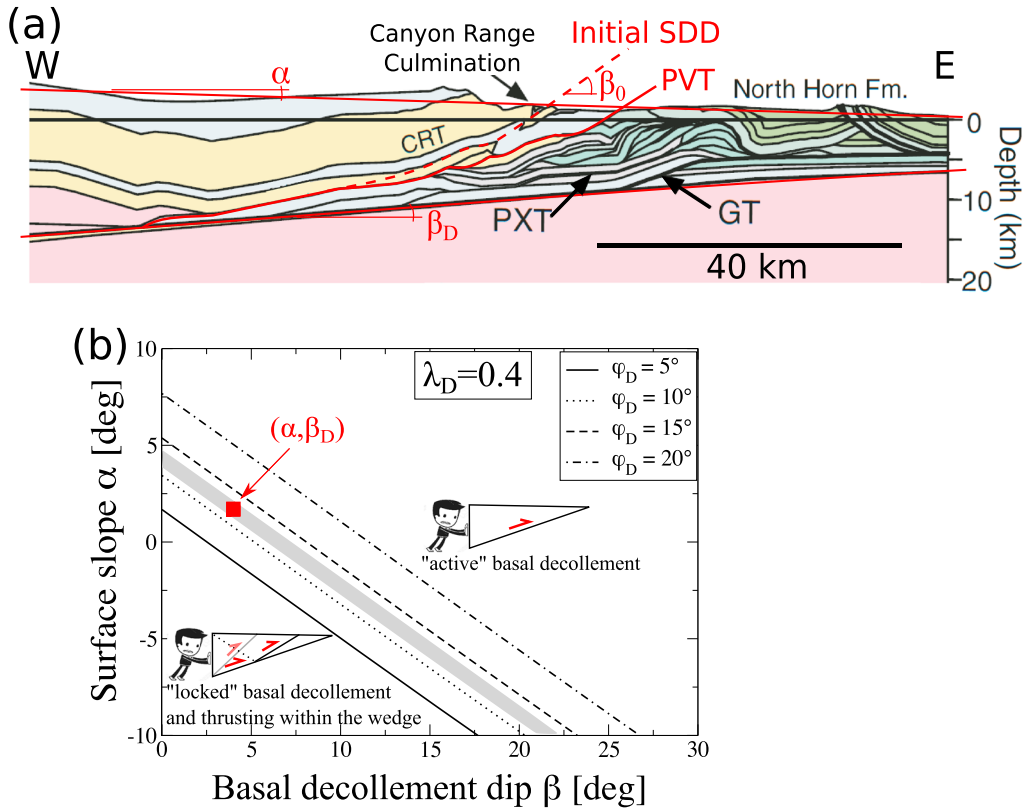

Figure 2. (a) Restoration of the Sevier thrust belt (modified from DeCelles & Coogan, 2006). (b) The relationship of surface slope to basal décollement dip at a critical wedge shape using compressive CCW theory (Dahlen, 1984) for a range of friction angles φ_D = 5° (μ_D = 0.09), 10° (0.18), 15° (0.27), and 20° (0.36), assuming hydrostatic fluid pressures on the décollement (fluid-pressure ratio λ_D = 0.4). In (b), the red square represents the geometry (α, β_D) of the décollement based upon preextensional structural constraints. The surface slope is positive for surface slope toward the wedge tip.

have reduced the surface slope. We assume that the average surface slope decreased from α = 1.7°, with uncertainty 0.3°, in the Miocene to the present-day topography. The detachment dip decreased from β_0 ~ 30° to 11°.

4. Modeling Results From Compressive CCW Theory

For most crustal rocks the friction coefficient is 0.85 at low pressure and 0.6 at greater pressure, where some cohesion is also needed (Byerlee, 1978). It has become common to use a single simple expression as $\tau = 0.6\sigma_n$, where τ and σ_n are shear traction and normal traction, respectively. Use of μ_B = 0.85 within the wedge would not greatly increase the friction coefficient that is inferred for the décollement. Additionally, the use of μ_B = 0.6 is more consistent with Anderson's theory of faulting, and the inclination of faults at ~60° in extensional settings. In modeling exercises using CCW theory, the wedge bulk material is assumed homogeneous and its internal friction angle φ_B is assumed to be 30° (μ_B ~ 0.58) consistent with the above expectations for upper crustal rocks. The basal décollement friction angle φ_D is the objective of this exercise. The décollement friction angles φ_D are set to 5° (μ_D = 0.09), 10° (0.18), 15° (0.27), and 20° (0.36). We assume that the bulk material and the décollement are cohesionless for the use of CCW theory. We also assume that the fluid pressure is hydrostatic ($\lambda_B = \lambda_D = \rho_f/\rho$ = 0.4) within the bulk material and on the décollement. It is a general assumption because the determination of effective friction coefficient μ_D' will be same even if the décollement is associated with fluid overpressure. The effective friction coefficient (equation (16) of Yuan et al., 2017) of the décollement is used here

$$\mu_D' = \frac{\tan(\varphi_D)(1-\lambda_D)}{1-\rho_f/\rho}. \quad (5)$$

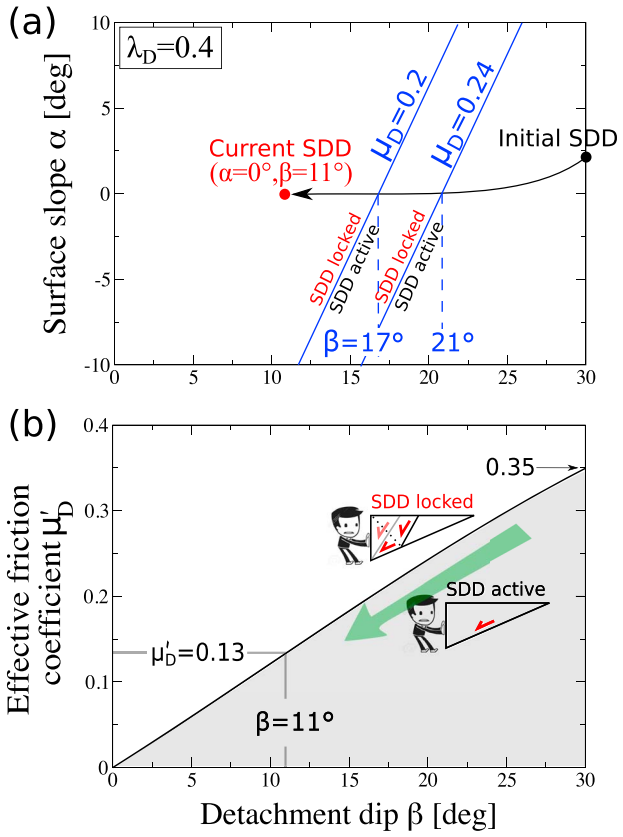

Figure 3. (a) Analysis of extensional CCW theory assuming hydrostatic fluid pressures on the SDD (λ_D = 0.4). The geometry (α, β) implied by the field to the left of the stability curve corresponds with a locked detachment. Geometry to the right of the curve corresponds with the extensional wedge slipping on an active detachment. The black curve with arrow shows approximately the changes of the wedge geometry during extension. (b) Stability map (detachment effective friction coefficient μ'_D versus detachment dip β) of active/locked SDD. For partly locked or fully locked SDD (cartoon in b), the wedge slips at depth instead of the whole detachment.

The value of μ'_D is valid for hydrostatic case, $\mu'_D = \mu_D = \tan(\varphi_D)$ when the value of λ_D is equal to ρ_f/ρ.

According to compressive CCW theory (Dahlen, 1984), if surface slope and décollement dip place wedge parameters in subcriticality, then thrust faulting will occur within the wedge, increasing the surface slope until the critical slope α_c is attained. Compressive CCW theory was used to constrain the décollement friction angle φ_D based on the Mesozoic structures above the basal décollement (Figure 2a). To ensure the nearly critical wedge above the décollement, the décollement friction angle φ_D (and corresponding friction coefficient) needs to be 12.5 ± 1° (0.2–0.24), as shown by the shading in Figure 2b.

5. Modeling Results From Extensional CCW Theory

We use extensional CCW theory (Xiao et al., 1991) to investigate the frictional properties that permit slip on the SDD and the reactivated PVT, as the cross section evolved from its preextensional (Figure 2a) to present-day arrangement (Figure 1a). Tests are shown in Figure 3a, again assuming hydrostatic fluid pressure ($\lambda_D = \rho_f/\rho$) on the basal décollement, which evolves into the detachment during subsequent extension.

The detachment dip decreased from $\beta_0 \sim 30°$ to the present-day dip of 11° as a result of isostatic rebound (black curve, Figure 3a). If the SDD has the same frictional characteristics (φ_D = 12.5 ± 1°, 0.2–0.24) as the décollement predicted from compressive CCW theory, the slip with the active SDD is possible only if the historical detachment dip $\beta \geq 21°$ for μ_D = 0.24, or $\beta \geq 17°$ for μ_D = 0.2 (Figure 3a). The failure mode (active or locked SDD) depends on how the geometry changed due to crustal thinning and isostatic rebound as a function of time.

If the SDD were well defined in the above range at the present time, it should be locked (Figure 3a). However, as noted in Christie-Blick et al. (2009), and indicated explicitly in DeCelles and Coogan (2006), high-angle normal faults are interpreted to terminate downward into the SDD. Those faults offset lake sediments as young as 8 ka (Oviatt, 1989). So one interpretation is that the downdip portion of the SDD was slipping as recently as 8 kyr ago with a dip of 11°, consistent with Global Positioning System evidence for extension across the Sevier Desert (Niemi et al., 2004; cf. Stahl & Niemi, 2017). Two mechanisms can be considered for permitting slip at such a low dip: fluid overpressure, and especially weak materials along the SDD.

We use the effective friction coefficient μ'_D in equation (5) to characterize the mechanical properties of detachment associated with fluid overpressure ($\rho_f/\rho < \lambda_D < 1$). The value of μ'_D as a function of detachment dip β is shown in Figure 3b where the shading shows the domain for an active SDD. A value of μ'_D lower than 0.35 is consistent with slip on the SDD during the initial extension ($\beta_0 \sim 30°$). For the present-day active SDD, the value of μ'_D should be lower than 0.13 (Figure 3b).

5.1. Weak Materials (Gouge and Salt)

The value of μ'_D may have decreased as a function of time, as implied in Figure 3b. We constrain an initial value of 0.2–0.24 on the basis of the compressive CCW calculation for preextensional thrust faults. The weakening process may have occurred during thrusting, and it may continue weakening the detachment during extension to as low as 0.13. A comparison with frictional coefficients for the weakest materials encountered in the SAFOD hole—μ'_D as low as ~0.11 in Coble et al. (2014), and in the range of 0.07–0.11 in Suppe (2007)—suggests that the SDD could have slipped at a dip of 11°. Similar weak LANFs include ancient exposed examples such as the Zuccale fault in Italy where the nature and mechanical properties of fault rocks can be examined both in the field (e.g., Collettini & Holdsworth, 2004; Smith et al., 2011; and references

therein) and in laboratory friction experiments (e.g., Collettini et al., 2009). Studies like this have shown very clearly that fault rocks associated with natural LANFs are indeed very weak with friction coefficients as low as 0.1. This can be due to the presence of weak minerals such as talc or smectite and/or to the operation of diffusion-accommodated frictional viscous creep. Reference to these examples instead of or as well as SAFOD would seem logical given that they are also LANFs. Collettini and Holdsworth (2004) and Collettini (2011) have pointed out that if LANFs are very weak, then it is not surprising that there are so few large magnitude earthquakes associated with such faults. Such faults would be expected to creep perhaps with numerous microseismic events, and this does seem to be consistent with the behavior of known currently active LANFs such as the Altotiberina fault in Italy (e.g., Chiaraluce et al., 2007).

Among obviously weak materials that might have been utilized in the Sevier Desert example is salt of Jurassic age and within the lake sediments of the late Cenozoic basin (e.g., Christie-Blick et al., 2007; Mitchell, 1979; Standlee, 1982; Wills et al., 2005). Davis and Engelder (1985) pointed out that salt would behave ductilely at depths in excess of 2 km, and perhaps much less than that. Widespread normal faulting above the SDD relates at least in part to Cenozoic salt (Wills et al., 2005). For a ductile detachment, CCW theory is also applicable since Davis et al. (1983) and Davis and Engelder (1985) suggest an approximate CCW theory by calculating an equivalent friction coefficient μ_D' to mimic the same yield shear stress ($\tau_D \leq 1$ MPa) along the detachment as a ductile layer.

5.2. Fluid Overpressure

Fluid overpressure appreciably greater than hydrostatic is not expected in fully lithified Proterozoic and Paleozoic strata or late Cenozoic lake sediments of the Sevier Desert basin in the upper few kilometers of the crust. It is, however, very common for pore fluid pressures to be hydrostatic at shallow depths and overpressured at deeper depths (Dahlen, 1990; Suppe, 2014). So we explore the possibility that overpressure is involved in detachment.

The friction coefficient determined from compressive CCW theory is in the range of 0.2–0.24, allowing slip on the SDD with a dip $\beta \geq 17°$ to 21°. Burial of the active SDD by clastic sediments to a depth of 3–5 km may have allowed detachment fluid pressure to exceed hydrostatic. Borehole data and seismic velocity analysis suggest that pore fluids in many clastic sedimentary basins become overpressured below a fluid-retention depth (Suppe, 2014). A decrease in the friction coefficient from 0.2 to 0.13 is equivalent to an increase in fluid pressure from hydrostatic ($\lambda_D = 0.4$) to overpressured ($\lambda_D = 0.62$), a value that is at least plausible in the Sevier Desert. Fluid overpressure can also develop at elevated temperature. For example, the experiments of Parry and Bruhn (1986) show that the pore fluid pressure on the Wasatch fault, a prominent normal fault to the east of the Sevier Desert, is greater than hydrostatic at a depth of ~5 km and a temperature of >160 °C (assuming a geothermal gradient of 30 °C/km). The present-day geothermal gradient beneath much of the SDD appears to be as high as 60–70 °C/km (Blackett et al., 2013). An intriguing possibility is that volcanic activity has raised the geothermal gradient since the Pleistocene to such a degree that the SDD is now ductile at depths as shallow as ~4 km.

Fluids weaken faults in another way, by promoting the growth of clay-rich coatings, which lower fault friction (e.g., Schleicher et al., 2010). Such clay gouges are common in carbonate-dominated fold and thrust belts (such as the Sevier) where pressure solution preferentially dissolves carbonate and concentrates clay, resulting in shear zones and faults with very low frictional coefficients (Lacroix et al., 2015). For the LANF in the Panamint Valley, California, experimental studies have shown that fault gouges with greater than 50 wt % clay content are generally in a range of $\mu_D = 0.2–0.4$, and certain fault gouges have a friction coefficient less than 0.2 (Numelin et al., 2007). Water-dampened smectite-rich gouges are weaker ($\mu_D' < 0.1$) than room-humidity gouges (μ_D = ~0.1–0.35) at all slip velocities (Remitti et al., 2015). If the SDD is associated with clay-rich gouge, the value of μ_D' could be lower than 0.13.

5.3. Cohesion

We assume for the purpose of this analysis that the Sevier orogen and Sevier Desert basin were effectively cohesionless during deformation. It is likely, however, that the thrust belt upper plate, made mainly of well cemented, fully compacted Proterozoic clastic rocks and Paleozoic carbonate rocks, was not so riddled with faults that intact rock strength can be ignored (see Axen, 2004; Axen & Selverstone, 1994). Estimated values of rock cohesion vary between 10 and 20 MPa for sedimentary rocks (Handin, 1966). Any amount of wedge

cohesion in the upper plate would increase the calculated value of μ_D', whereas any amount of detachment cohesion would decrease this value. How wedge and detachment cohesions may have influenced our results remains to be evaluated quantitatively. An approach developed by Yuan et al. (2015) suggests a possible way forward. Assuming a cohesionless detachment, a first order of wedge cohesion of 20 MPa would increase the value of μ_D' from 0.13 (lower bound) to ~0.2 (upper bound).

6. Conclusion

The SDD is of broad interest because for more than 40 years it has represented a benchmark for the interpretation of regional detachment faults everywhere. We have explored the paradox of low-angle normal faulting in the Sevier Desert of west-central Utah by considering the range of friction coefficients implied by the interpretation of a regional-scale extensional detachment. Compressive CCW theory suggests μ_D values of 0.2–0.24 for thrust faults when crustal shortening ceased in the early Paleocene. Extensional CCW theory implies that the effective friction coefficient of the detachment decreased to ~0.13. The weakening process may have occurred during thrusting, which could be precondition of further weakening the detachment during extension to as low as 0.13. This may have been due to the involvement of weak materials such as salt or clay-rich gouge or to a modest increase in pore fluid pressure (λ_D ~ 0.6, 60% of the lithostatic pressure). Our results can be tested by coring across the inferred detachment and by measuring material properties and the pore fluid pressure in the vicinity of the contact. Our findings can also be compared with observations at active subduction megathrusts sampled by the Integrated Ocean Drilling Program and other deep drilling programs where similar weakening mechanisms may also have been involved.

Acknowledgments
We thank Gary Axen, Jon Spencer, an anonymous reviewer, the Associate Editor, and Editor Jeroen Ritsema for their helpful reviews, and Bob Holdsworth's review for initial version. Lamont-Doherty Earth Observatory contribution number 8203. This paper is based on published data and on a theoretical approach presented in Yuan et al. (2015).

References

Allmendinger, R. W., Sharp, J. W., Von Tish, D., Serpa, L., Brown, L., Kaufman, S., et al. (1983). Cenozoic and Mesozoic structure of the eastern Basin and Range province, Utah, from COCORP seismic-reflection data. *Geology*, *11*(9), 532–536. https://doi.org/10.1130/0091-7613(1983)11%3C532:CAMSOT%3E2.0.CO;2

Anders, M. H., Christie-Blick, N., & Malinverno, A. (2012). Cominco American well: Implications for the reconstruction of the Sevier orogen and basin and range extension in west-central Utah. *American Journal of Science*, *312*(5), 508–533. https://doi.org/10.2475/05.2012.02

Anders, M. H., Christie-Blick, N., Wills, S., & Krueger, S. W. (2001). Rock deformation studies in the Mineral Mountains and Sevier Desert of west-central Utah: Implications for upper crustal low-angle normal faulting. *Geological Society of America Bulletin*, *113*(7), 895–907. https://doi.org/10.1130/0016-7606(2001)113%3C0895:RDSITM%3E2.0.CO;2

Axen, G. J. (2004). Mechanics of low-angle normal faults. In G. D. Karner, B. Taylor, N. W. Driscoll, & D. L. Kohlstedt (Eds.), *Rheology and deformation of the lithosphere at continental margins* (pp. 46–91). New York: Columbia University Press. https://doi.org/10.7312/karn12738-004

Axen, G. J., & Bartley, J. M. (1997). Field tests of rolling hinges: Existence, mechanical types, and implications for extensional tectonics. *Journal of Geophysical Research*, *102*(B9), 20,515–20,537. https://doi.org/10.1029/97JB01355

Axen, G. J., & Selverstone, J. (1994). Stress-state and fluid-pressure level along the Whipple detachment fault, California. *Geology*, *22*(9), 835–838. https://doi.org/10.1130/0091-7613(1994)022%3C0835:SSAFPL%3E2.3.CO;2

Blackett, R., Gwynn, M., Hardwick, C., Thomas, K., Weaver, L., & Allis, R. (2013). Utah contributions to the national geothermal data system. *GRC Transactions*, *37*, 559–563.

Buck, W. R. (1988). Flexural rotation of normal faults. *Tectonics*, *7*(5), 959–973. https://doi.org/10.1029/TC007i005p00959

Byerlee, J. (1978). Friction of rocks. *Pure and Applied Geophysics*, *116*(4-5), 615–626. https://doi.org/10.1007/BF00876528

Chiaraluce, L., Chiarabba, C., Collettini, C., Piccinini, D., & Cocco, M. (2007). Architecture and mechanics of an active low-angle normal fault: Alto Tiberina fault, northern Apennines, Italy. *Journal of Geophysical Research*, *112*, B10310. https://doi.org/10.1029/2007JB005015

Christie-Blick, N., Anders, M. H., Manatschal, G., & Wernicke, B. P. (2009). Testing the extensional detachment paradigm: A borehole observatory in the Sevier Desert basin. *Scientific Drilling*, *8*, 57–59. https://doi.org/10.2204/iodp.sd.8.09.2009

Christie-Blick, N., Anders, M. H., Wills, S., Walker, C. D., & Renik, B. (2007). Observations from the Basin and Range Province (western United States) pertinent to the interpretation of regional detachment faults. *Geological Society, London, Special Publications*, *282*(1), 421–441. https://doi.org/10.1144/SP282.17

Coble, C., French, M., Chester, F., Chester, J., & Kitajima, H. (2014). In situ frictional properties of San Andreas Fault gouge at SAFOD. *Geophysical Journal International*, *199*(2), 956–967. https://doi.org/10.1093/gji/ggu306

Collettini, C. (2011). The mechanical paradox of low-angle normal faults: Current understanding and open questions. *Tectonophysics*, *510*(3-4), 253–268. https://doi.org/10.1016/j.tecto.2011.07.015

Collettini, C., & Holdsworth, R. E. (2004). Fault zone weakening and character of slip along low-angle normal faults: Insights from the Zuccale fault, Elba, Italy. *Journal of the Geological Society*, *161*(6), 1039–1051. https://doi.org/10.1144/0016-764903-179

Collettini, C., Niemeijer, A., Viti, C., & Marone, C. (2009). Fault zone fabric and fault weakness. *Nature*, *462*(7275), 907–910. https://doi.org/10.1038/nature08585

Collettini, C., & Sibson, R. H. (2001). Normal faults, normal friction? *Geology*, *29*(10), 927–930. https://doi.org/10.1130/0091-7613(2001)029%3C0927:NFNF%3E2.0.CO;2

Dahlen, F. A. (1984). Noncohesive critical Coulomb wedges: An exact solution. *Journal of Geophysical Research*, *89*(B12), 10,125–10,133. https://doi.org/10.1029/JB089iB12p10125

Dahlen, F. A. (1990). Critical taper model of fold-and-thrust belts and accretionary wedges. *Annual Review of Earth and Planetary Sciences*, *18*(1), 55–99. https://doi.org/10.1146/annurev.ea.18.050190.000415

Davis, D., Suppe, J., & Dahlen, F. A. (1983). Mechanics of fold-and-thrust belts and accretionary wedges. *Journal of Geophysical Research*, *88*(B2), 1153–1172. https://doi.org/10.1029/JB088iB02p01153

Davis, D. M., & Engelder, T. (1985). The role of salt in fold-and-thrust belts. *Tectonophysics*, *119*(1-4), 67–88. https://doi.org/10.1016/0040-1951(85)90033-2

DeCelles, P. G., & Coogan, J. C. (2006). Regional structure and kinematic history of the Sevier fold-and-thrust belt, central Utah. *Geological Society of America Bulletin*, *118*(7-8), 841–864. https://doi.org/10.1130/B25759.1

DeCelles, P. G., & Mitra, G. (1995). History of the Sevier orogenic wedge in terms of critical taper models, northeast Utah and southwest Wyoming. *Geological Society of America Bulletin*, *107*(4), 454–462. https://doi.org/10.1130/0016-7606(1995)107%3C0454:HOTSOW%3E2.3.CO;2

Forsyth, D. W. (1992). Finite extension and low-angle normal faulting. *Geology*, *20*(1), 27–30. https://doi.org/10.1130/0091-7613(1992)%E2%80%8B020%3C0027:FEALAN%3E%E2%80%8B2.3.CO;2

Gregory-Wodzicki, K. M. (1997). The late Eocene House Range Flora, Sevier Desert, Utah: Paleoclimate and paleoelevation. *PALAIOS*, *12*(6), 552–567. https://doi.org/10.2307/3515411

Handin, J. (1966). Strength and ductility. In S. P. Clark, Jr. (Ed.), *Handbook of Physical Constants, Memoir* (pp. 223–289). New York: Geological Society of America. https://doi.org/10.1130/MEM97-p223

Jackson, J. A., & White, N. J. (1989). Normal faulting in the upper continental crust: Observations from regions of active extension. *Journal of Structural Geology*, *11*(1-2), 15–36. https://doi.org/10.1016/0191-8141(89)90033-3

Lacroix, B., Tesei, T., Oliot, E., Lahfid, A., & Collettini, C. (2015). Early weakening processes inside thrust fault. *Tectonics*, *34*(7), 1396–1411. https://doi.org/10.1002/2014TC003716

Lister, G. S., Etheridge, M. A., & Symonds, P. A. (1991). Detachment models for the formation of passive continental margins. *Tectonics*, *10*(5), 1038–1064. https://doi.org/10.1029/90TC01007

Manatschal, G., Muntener, O., Lavier, L., Minshull, T., & Péron-Pinvidic, G. (2007). Observations from the Alpine Tethys and Iberia–Newfoundland margins pertinent to the interpretation of continental breakup. In G. D. Karner, G. Manatschal, & L. M. Pinheiro (Eds.), *Imaging, Mapping and Modelling Continental Lithosphere Extension and Breakup*, *Geological Society, London, Special Publications* (Vol. 282, pp. 291–324). https://doi.org/10.1144/SP282.14

McBride, J. H., Stephenson, W. J., & McBride, E. I. P. (2010). Reanalysis of the COCORP Utah Line 1 deep seismic reflection profile: Toward an improved understanding of the Sevier Desert detachment question. *Geosphere*, *6*(6), 840–854. https://doi.org/10.1130/GES00546.1

Mesimeri, M., Karakostas, V., Papadimitriou, E., Tsaklidis, G., & Jacobs, K. (2018). Relocation of recent seismicity and seismotectonic properties in the Gulf of Corinth (Greece). *Geophysical Journal International*, *212*, 1123–1142.

Mitchell, G. C. (1979). Stratigraphy and regional implications of the Argonaut Energy No. 1 Federal, Millard County, Utah. Basin and Range Symposium (pp. 503–514). Rocky Mountain Association of Geologists, Utah Geological Association.

Niemi, N. A., Wernicke, B. P., Friedrich, A. M., Simons, M., Bennett, R. A., & Davis, J. L. (2004). BARGEN continuous GPS data across the eastern Basin and Range province, and implications for fault system dynamics. *Geophysical Journal International*, *159*(3), 842–862. https://doi.org/10.1111/j.1365-246X.2004.02454.x

Numelin, T., Marone, C., & Kirby, E. (2007). Frictional properties of natural fault gouge from a low-angle normal fault, Panamint Valley, California. *Tectonics*, *26*, TC2004. https://doi.org/10.1029/2005TC001916

Oviatt, C. G. (1989). *Quaternary geology of part of the Sevier Desert, Millard County, Utah*, *Utah Geological and Mineral Survey Special Studies* (Vol. 70, p. 41). Salt Lake City, Utah: Utah Department of Natural Resources.

Parry, W., & Bruhn, R. (1986). Pore fluid and seismogenic characteristics of fault rock at depth on the Wasatch fault, Utah. *Journal of Geophysical Research*, *91*(B1), 730–744. https://doi.org/10.1029/JB091iB01p00730

Proffett, J. M. (1977). Cenozoic geology of the Yerington district, Nevada, and implications for the nature and origin of Basin and Range faulting. *Geological Society of America Bulletin*, *88*(2), 247–266. https://doi.org/10.1130/0016-7606(1977)88%3C247:CGOTYD%3E2.0.CO;2

Remitti, F., Smith, S. A. F., Mittempergher, S., Gualtieri, A. F., & Di Toro, G. (2015). Frictional properties of fault zone gouges from the J-FAST drilling project (Mw 9.0 2011 Tohoku-Oki earthquake). *Geophysical Research Letters*, *42*, 2691–2699. https://doi.org/10.1002/2015GL063507

Schleicher, A. M., van der Pluijm, B. A., & Warr, L. N. (2010). Nanocoatings of clay and creep of the San Andreas fault at Parkfield, California. *Geology*, *38*(7), 667–670. https://doi.org/10.1130/G31091.1

Sibson, R. H. (1985). A note on fault reactivation. *Journal of Structural Geology*, *7*(6), 751–754. https://doi.org/10.1016/0191-8141(85)90150-6

Smith, S. A. F., Holdsworth, R. E., Collettini, C., & Pearce, M. A. (2011). The microstructural character, evolution and mechanical significance of fault rocks associated with a continental low-angle normal fault: The Zuccale fault, Elba Island, Italy. In A. Fagereng, V. G. Toy, & J. V. Rowland (Eds.), *Geology of the earthquake source: A volume in honour of Rick Sibson*, *Geological Society, London, Special Publications* (Vol. 359, pp. 97–113). https://doi.org/10.1144/SP359.6

Stahl, T., & Niemi, N. A. (2017). Late quaternary faulting in the Sevier Desert driven by magmatism. *Scientific Reports*, *7*, 44,372. https://doi.org/10.1038/srep44372

Standlee, L. A. (1982). Structure and stratigraphy of Jurassic rocks in central Utah: Their influence on tectonic development of the Cordilleran foreland thrust belt. In *Geologic Studies of the Cordilleran Thrust Belt*, *Rocky Mountain Association of Geologists* (Vol. I, pp. 357–382). Denver: CO.

Suppe, J. (2007). Absolute fault and crustal strength from wedge tapers. *Geology*, *7*(6), 751–754. https://doi.org/10.1016/0191-8141(85)90150-6

Suppe, J. (2014). Fluid overpressures and strength of the sedimentary upper crust. *Journal of Structural Geology*, *69*, 481–492. https://doi.org/10.1016/j.jsg.2014.07.009

Von Tish, D. B., Allmendinger, R. W., & Sharp, J. W. (1985). History of Cenozoic extension in central Sevier Desert, west-central Utah, from COCORP seismic reflection data. *AAPG Bulletin*, *69*, 1077–1087.

Wernicke, B. (1985). Uniform-sense normal simple shear of the continental lithosphere. *Canadian Journal of Earth Sciences*, *22*(1), 108–125. https://doi.org/10.1139/e85-009

Wernicke, B., & Axen, G. J. (1988). On the role of isostasy in the evolution of normal fault systems. *Geology*, *16*(9), 848–851. https://doi.org/10.1130/0091-7613(1988)016%3C0848:OTROII%3E2.3.CO;2

Whitney, D. L., Teyssier, C., Rey, P., & Buck, W. R. (2013). Continental and oceanic core complexes. *Geological Society of America Bulletin*, *125*(3-4), 273–298. https://doi.org/10.1130/B30754.1

Wills, S., Anders, M. H., & Christie-Blick, N. (2005). Pattern of Mesozoic thrust surfaces and Tertiary normal faults in the Sevier Desert subsurface, west-central Utah. *American Journal of Science*, *305*(1), 42–100. https://doi.org/10.2475/ajs.305.1.42

Xiao, H.-B., Dahlen, F. A., & Suppe, J. (1991). Mechanics of extensional wedges. *Journal of Geophysical Research*, *96*(B6), 10,301–10,318. https://doi.org/10.1029/91JB00222

Yuan, X. P., Leroy, Y. M., & Maillot, B. (2015). Tectonic and gravity extensional collapses in overpressured cohesive and frictional wedges. *Journal of Geophysical Research: Solid Earth*, *120*, 1833–1854. https://doi.org/10.1002/2014JB011612

Yuan, X. P., Leroy, Y. M., & Maillot, B. (2017). Reappraisal of gravity instability conditions for offshore wedges: Consequences for fluid overpressures in the Niger Delta. *Geophysical Journal International*, *208*, 1655–1671. https://doi.org/10.1093/gji/ggw474